AC response of fractal metal-electrolyte interfaces

1994 J. Phys.: Condens. Matter 6 10509

(http://iopscience.iop.org/0953-8984/6/48/012)

J. Phys.: Condens. Matter 6 (1994) 10509–10517. Printed in the UK

AC response of fractal metal–electrolyte interfaces

H Ruiz-Estrada†, R Blender‡ and W Dieterich
Fakultät für Physik, Universität Konstanz, Universitätsstrasse 10, D-78464 Konstanz, Germany

Received 21 April 1994, in final form 12 September 1994

Abstract. The problem of the so-called constant phase angle (CPA) behaviour in the frequency-dependent impedance of an electrolyte in contact with a rough metallic electrode is studied by a numerical treatment and by real-space renormalization of two-dimensional electrical networks. Deterministic and disordered fractal boundaries based on quadratic Koch curves are considered. Both methods indicate that the CPA exponent η can be estimated qualitatively from both the fractal dimension of the interface and from the scaling of the high-frequency response with system size.

1. Introduction

The low-frequency impedance ($\nu \leqslant 10^5$ Hz) of liquid or solid electrolytes in contact with a metallic electrode typically shows an anomalous frequency dependence, often represented as a power law $Z(\omega) - Z(\infty) \propto (i\omega)^{-\eta}$. In the ideal case of a perfectly planar electrode, one expects an impedance corresponding to the electrolyte resistance in series with a double-layer capacitance, and hence $\eta = 1$. Experiments, however, often yield exponents $0 < \eta < 1$ over several decades of frequency, a behaviour known as the 'constant phase angle (CPA)' response and usually attributed to irregularities in the interfacial geometry. The relationship between the dynamic exponent η and the geometry of a rough interface has been subject to much attention in recent years. In particular, the idea that disordered structures can often be modelled by fractals has initiated a number of studies of fractal electrodes (Le Méhauté and Crepy 1983; for a review and recent literature, see Sapoval 1991).

Theoretically, one may use a discretized description and start from an equivalent circuit containing constant conductances σ_b within the electrolyte region and conductance elements $\sigma_i = i\omega C$, C being the double-layer capacitance per unit area, which connect the electrolyte with the electrode. This is, of course, a poor description of real electrolyte–electrode processes. However, such models account for the essential aspect that, in the presence of a voltage $V(t) = V_0 e^{i\omega t}$ applied to the system, different frequencies ω will explore different geometrical characteristics of the fractal interface. Clearly, at high frequencies, those parts of the electrode that are closest to the counter-electrode will carry most of the current, whereas remote parts will be shielded. By lowering the frequency, the equipotential surfaces will penetrate the deeper cavities, which in turn participate in the current transport. The multifractal nature of the resulting electrostatic potential problem has been emphasized recently by Geertsma *et al* (1989) and by Halsey and Leibig (1991). Therefore, in general, one cannot expect that η is a function of merely the fractal dimension D of the interface.

† Present address: Universidad Autónoma de Puebla, av. San Claudio y 14 Sur, 72000 Puebla, Mexico.
‡ Universität Hamburg, Meteorologisches Institut, Bundesstrasse 55, D-20146 Hamburg, Germany.

0953-8984/94/4810509+09$19.50

Numerical studies of these questions for two-dimensional systems essentially followed two different routes. Blender *et al* (1990) considered a quadratic Koch curve with $D = 1.5$ and solved for the complex electrostatic potential by a relaxation method. From calculations up to stage $N = 4$ in the fractal construction they found a dynamic impedance whose imaginary part is well represented by a power law within about three decades in frequency. The exponent was found to be $\eta \simeq 0.6$ and therefore close to but significantly smaller than that expected from the relation $\eta = D^{-1}$, which was suggested previously (Le Méhauté and Crepy 1983). Meakin and Sapoval (1991, 1992) and Sapoval *et al* (1993) exploited the formal analogy between electrostatic and random walk problems (Chandrasekhar 1943, Pietronero and Wiesmann 1984). Using the random walk approach they calculated the impedance along the real axis of σ_i values for electrodes of the form of diffusion-limited aggregation (DLA) clusters as well as for porous electrodes, and gave arguments that η is well approximated by $\eta \simeq 1/D$ in the case of DLA structures.

In this paper we again employ the relaxation method, where the calculated imaginary part $\mathrm{Im}\, Z(\omega)$ is directly sensitive to interfacial properties entering via the imaginary interface conductance $\sigma_i = \mathrm{i}\omega C$. This allows us to detect numerically a non-trivial scaling of the high-frequency impedance with respect to the system size. A simple interpolation scheme is proposed, wherein the exponent η is estimated from properties of the interface in the low- and high-frequency limit. This scheme is compared with calculations for the quadratic Koch-curve with $D = 1.5$ and modifications thereof, including disordered structures. Furthermore, we show that by a renormalization procedure using successively larger cells we obtain semiquantitative agreement with our numerical results.

2. Quadratic Koch boundary

In this section we study a two-dimensional model of an electrochemical cell consisting of an electrolyte between an electrode of the form of a quadratic Koch curve and a planar counter-electrode. In constructing our model we follow Blender *et al* (1990). The Koch electrode is generated as shown in figure 1(*a*) and has a fractal dimension $D = \ln 8/\ln 4 = 1.5$. At stage N ($N \geqslant 1$) in our construction we start from a square lattice of size $L \times L$ with $L = 4^N$ and incorporate the Koch curve as illustrated in figure 1(*b*) for both $N = 1$ and $N = 2$. Note that each of its elementary segments intersects one lattice bond, and these bonds are regarded as interface conductances $\sigma_i = \mathrm{i}\omega C$. Within the remaining bonds between the Koch electrode and the upper edge of the system (the counter-electrode) we associate constant (real) conductances σ_b, which represent the bulk electrolyte. Boundary conditions are chosen such that the counter-electrode, i.e. the lattice points in the upper edge of our lattice are held at a fixed potential $V = 1$, whereas $V = 0$ at the endpoints of interface bonds below the Koch electrode. Periodic boundary conditions are applied in the horizontal directions. The Kirchhoff equations for the network are solved by a relaxation method. It turns out that with an increasing number of iterations the total current calculated at the counter-electrode and the total current across the Koch electrode provide upper and lower bounds of the exact current, which tend to converge to a common limit. The iteration is continued until both quantities agree to within an error of about 10^{-3}.

Clearly, the impedance of the system at stage N can be written as $Z_N(\sigma_b, \sigma_i) = \sigma_b^{-1} f_N(\mathrm{i}x)$, where $x = \omega C/\sigma_b$. Data for its imaginary part are shown in figure 2 for $N = 2$ and $N = 4$. In accordance with previous findings (Blender *et al* 1990) three

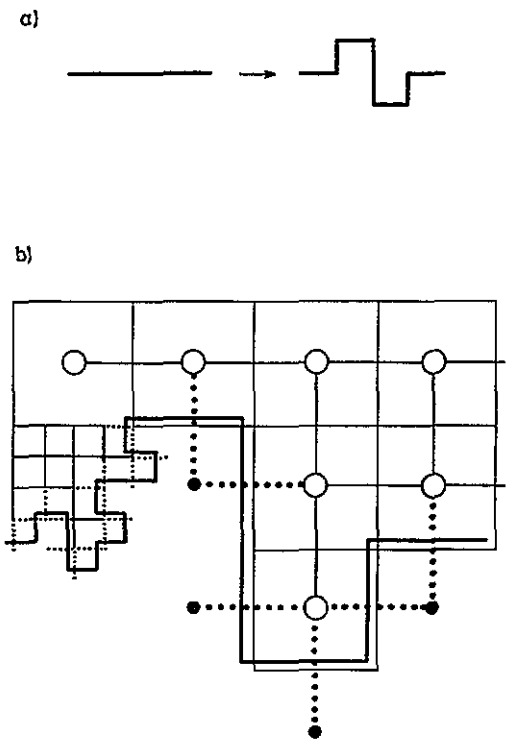

Figure 1. (*a*) Generation of the Koch curve electrode. (*b*) Electrical network of bulk conductances σ_b (——) and interface conductances σ_i (·····) across the Koch boundary at stage $N = 1$. One of the basic squares is subdivided according to stage $N = 2$.

regimes are clearly identified with the following characteristic behaviour of Im Z_N:

$$\sigma_b \mathrm{Im}\, Z_N \sim \begin{cases} (4^{DN}x)^{-1} & x \ll x_N^* \quad (1a) \\ (C_N x)^{-\eta} & x_N^* \ll x \ll 1 \quad (1b) \\ (B_N x)^{-1} & 1 \ll x. \quad (1c) \end{cases}$$

In the low-frequency regime the current is limited predominantly by the Koch interface and hence is simply proportional to the number of interface bonds, $8^N = 4^{DN}$. This leads immediately to (1*a*). The crossover to that regime occurs near the frequency ω_N^* determined by

$$x_N^* = \omega_N^* C/\sigma_b = 4^{-DN}. \quad (2)$$

Simultaneously we observe that Re Z_N saturates with decreasing frequency and also becomes independent of N.

In the intermediate 'anomalous' regime our results tend to follow a power law (1*b*), with an exponent $\eta < 1$ as N increases. For $N = 4$ an excellent fit is achieved with $\eta \simeq 0.60 \pm 0.01$ over about three orders of magnitude in frequency. Correspondingly, Re Z_N shows dispersion connecting its low- and high-frequency limits. Representative data points for Re Z_N with $N = 4$ are included in figure 4; see also the discussion in our previous work (Blender *et al* 1990).

Finally, for frequencies such that $x \gg 1$, we again have Re Z_N independent of N, whereas Im Z_N is given by (1*c*). We now analyse more closely the prefactor B_N. Calculations up to $N = 5$ in the high-frequency range indicate that as N increases, B_N/B_{N-1} tends to a constant that is smaller than 4. (In fact, we find $B_3/B_2 \simeq 3.87$, $B_4/B_3 \simeq 3.69$ and

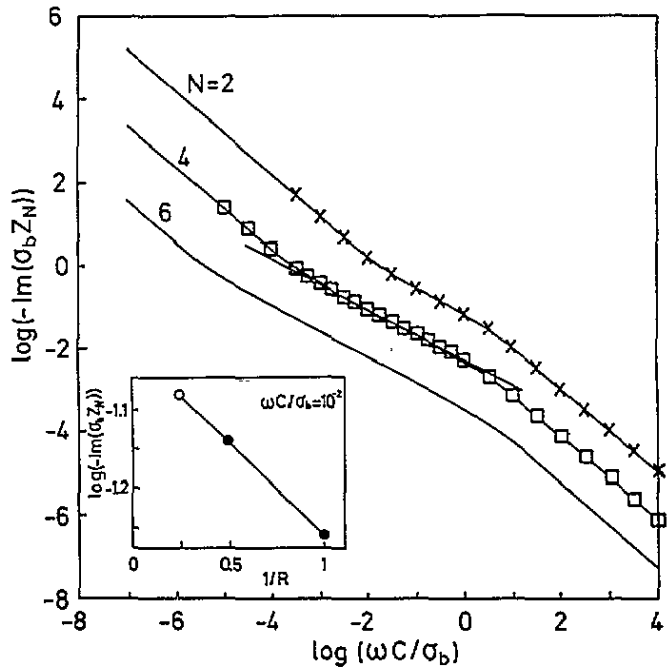

Figure 2. Imaginary part of the impedance against frequency. Data points are from numerical calculations for $N = 2$ (×) and $N = 4$ (□). Full curves are from an improved renormalization, see section 4, obtained by extrapolating first-order and second-order results as indicated in the inset. The straight line corresponds to a behaviour $\mathrm{Im}\, Z_N \sim \omega^{-0.60}$ of the data for $N = 4$.

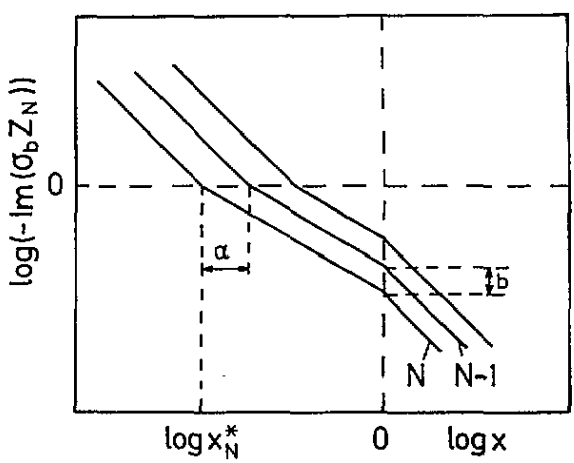

Figure 3. Illustration of our scheme of estimating η from the N dependence of the imaginary part $\mathrm{Im}\, Z_N$ at low and high frequencies.

$B_5/B_4 \simeq 3.66 \pm 0.1$.) With this hypothesis let us consider large N and define $B_N/B_{N-1} = 4^\tau$, or

$$B_N \simeq 4^{\tau N} \tag{3}$$

with $\tau \simeq 0.94 \pm 0.02$. Hence, for $x \gg 1$ fixed, $\log(-\sigma_b \mathrm{Im}\, Z_N) \simeq -Nb$ for large N, with $b = \tau \log 4$. Similarly, for $x \ll x_N^*$ fixed, $\log(-\sigma_b \mathrm{Im}\, Z_N) \simeq -Na$ for large

N, with $a = D\log 4$, see equation (1a). Since $\log x_N^* = -Na$ we are thus led to the following interpolation scheme for estimating η. From the behaviour of $\mathrm{Im}\, Z_N$ for large N schematically depicted in figure 3, it is obvious that the straight lines in the intermediate regime $x_N^* \ll x \ll 1$ have a slope $-\eta$ with $\eta = b/a$ or

$$\eta = \tau/D. \tag{4}$$

Thus η is expressed by two exponents: the fractal dimension, D, which enters via the low-frequency behaviour governed by the total length of the boundary, and the exponent, τ, related to the high-frequency regime, which is determined by the geometry of protrusions in the boundary. Using the above estimate for τ and $D = 1.5$, equation (3) predicts $\eta \simeq 0.62 \pm 0.01$, in remarkable agreement with the numerical value given above. Formally, continuity of $\mathrm{Im}\, Z_N$ at the two crossover frequencies $x = x_N^*$ and $x = 1$ suggests that instead of (1) we write

$$\sigma_b \mathrm{Im}\, Z_N \sim \begin{cases} x_N^*/x & x \ll x_N^* \quad (5a) \\ (x_N^*/x)^\eta & x_N^* \ll x \ll 1 \quad (5b) \\ (x_N^*)^\eta/x & 1 \ll x. \quad (5c) \end{cases}$$

In this form, the dependence of the impedance in the intermediate regime on N is made explicit, $C_N = 1/x_N^*$, and equation (5c) implies that $(x_N^*)^\eta B_N = 1$, which leads to equation (4). In fact, equation (4) agrees with a recent suggestion by Halsey and Leibig (1991). Their results, based on a Green function representation of the problem, imply a high-frequency expansion of the impedance, with the two leading terms ($x \to \infty$)

$$\sigma_b \mathrm{Re}\, Z_N \simeq \sigma_b \left(\sum_i j_i \right)^{-1} \tag{6}$$

and

$$\sigma_b \mathrm{Im}\, Z_N \simeq \frac{1}{x} \left(\sum_i (j_i)^2 \right) \left(\sum_i j_i \right)^{-2}. \tag{7}$$

Here the summation is over the endpoints i of interface bonds 'above' the boundary and j_i denotes the current entering i via bulk (electrolyte) conductances, which is derived from the electrostatic potential in the cell at infinite frequencies. Comparing (7) with (1c) and (3) it follows that B_N is proportional to the second moment of the 'harmonic measure' j_i, whose scaling with the system size $L = 4^N$ is characterized by the multifractal exponent $\tau(2)$, and thus we have $\tau \equiv \tau(2)$.

In connection with self-similar electrodes, attention has been drawn recently to the concept of the 'information fractal' (Sapoval *et al* 1993), which in our discrete case is the subset of interfacial points i that dominates the sum $\sum_i j_i$. For $d = 2$ its dimension is unity. This may reflect itself in the fact that $\mathrm{Re}\, Z(\omega \to \infty)$, determined by (6), becomes independent of L as in the case of non-fractal interfaces.

3. Generalized Koch boundaries

For a further test of the relation (4) we now investigate some modifications of the interfacial geometry. First, consider the modified generator in figure 4(a), where in comparison with

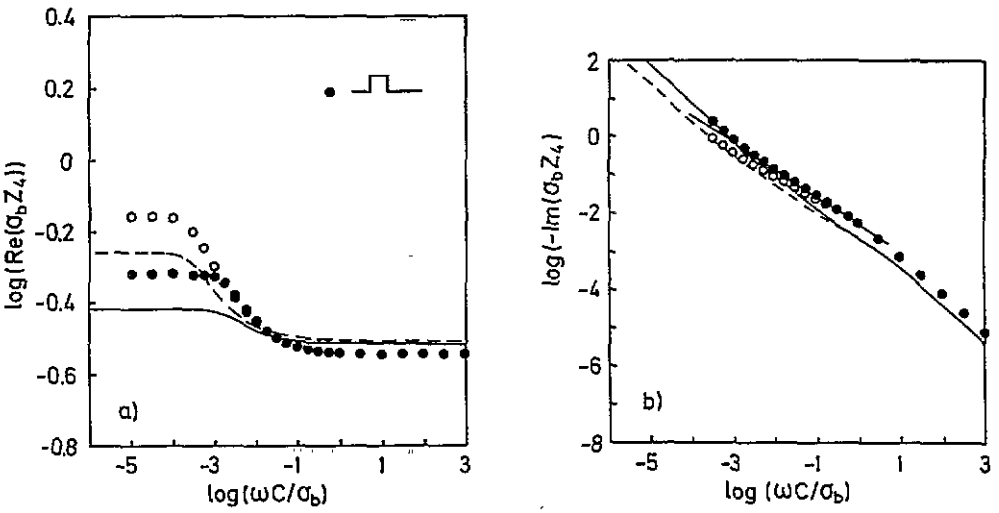

Figure 4. Real part (a) and imaginary part (b) of the impedance against frequency for the modified Koch fractal, see the generator in the inset, at $N = 4$ (full circles). The results according to the generator figure 1(a) are also shown for comparison (open circles). Full and open circles become indistinguishable for $\omega C/\sigma_b > 10^{-2}$. Full and broken curves, respectively, are the results from first-order renormalization, see section 4. The straight line in (b) has a slope $-\overline{\eta}$ with $\overline{\eta} = 0.70$.

figure 1(a) the cavity is removed. From the foregoing discussion we expect that the high-frequency behaviour of the impedance and therefore the exponent τ remain essentially unchanged in comparison with section 2, whereas the low-frequency behaviour is now given by (1a) with D replaced by $\overline{D} = \ln 6/\ln 4 \simeq 1.29$. Hence equation (4) predicts that $\overline{\eta} \simeq 0.73$. Numerical results for both $\mathrm{Re}\, Z_N$ and $\mathrm{Im}\, Z_N$ are plotted in figure 4 for $N = 4$. The corresponding data for the Koch boundary considered in section 2 are also shown for comparison and, indeed, both agree at high frequencies. Although the dispersive regime is reduced in the present case ($x_4^* \simeq 10^{-3}$), a power law fit, equation (1b), appears to be reasonable, which yields $\overline{\eta} \simeq 0.70 \pm 0.02$. This value is in good agreement with the above estimate.

Next we introduce structural disorder into our system. A disordered boundary is obtained by applying the generator of figure 1(a) with probability $(1 - p)$ to each of the smallest segments at a given stage N; with probability p the considered segment remains unchanged (see figure 5). The case $p = 0$ corresponds to the deterministic construction considered before. This procedure generates a family of boundaries whose dimension is approximately given by $D(p) = \ln[4p+4^D(1-p)]/\ln 4$, with $D \equiv D(0)$. For our numerical calculation we choose $p = 0.5$ and average the impedance over about 30 configurations of the boundary. From a set of data in the dispersive regime, see figure 5, we find $\eta(p) \simeq 0.72 \pm 0.02$. In a similar way we randomize the modified generator of figure 4(a). The result for the CPA exponent in that case is $\overline{\eta}(p) \simeq 0.81 \pm 0.02$. Assuming again the same high-frequency behaviour in both of these cases, we expect from (4) a ratio $\eta(p)/\overline{\eta}(p) = \overline{D}(p)/D(p) \simeq 0.9$ for $p = 0.5$, in good agreement with the numerical values for $\eta(p)$ and $\overline{\eta}(p)$ given above.

4. Position-space renormalization

The self-similar structure of the Koch boundary in our model of section 2 suggests the

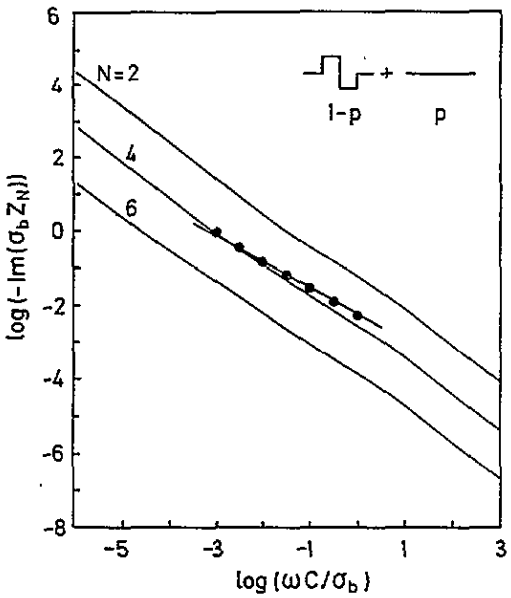

Figure 5. Generation of randomized Koch fractals and the corresponding impedance obtained from a first-order simulation for $N = 4$ (data points) and from renormalization (full curves, see section 4). The straight line has a slope -0.72.

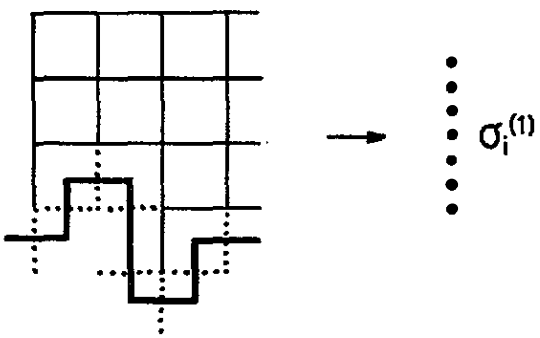

Figure 6. Definition of the renormalized (first-order) interface conductance $\sigma_i^{(1)}$.

application of suitable renormalization schemes. A simple but efficient scheme, which we call here first-order renormalization, has been proposed previously by Blender *et al* (1990). Here, let us recall it briefly and then generalize it to larger cells and also to disordered boundaries.

First, it is straightforward to calculate exactly the conductance $\Sigma_1(\sigma_i) = Z_1^{-1}$ for general complex arguments. Next, our system at stage N is mapped onto a system at stage $(N-1)$, which involves a renormalized interface conductance $\sigma_i^{(1)}$. Thereby the bulk conductance remains unchanged. The transformed conductance $\sigma_i^{(1)}$ should represent the conductance properties of a 4×4 cell connected to the interface. Hence we approximate it by the conductance of the cell shown in figure 6 in the vertical direction. After $(N-1)$ iterations we thus obtain a renormalized conductance $\sigma_i^{(N-1)}$. Finally, we can write the approximate relation

$$Z_N^{-1} = \Sigma_1\left(\sigma_i^{(N-1)}\right) \tag{8}$$

which for large N was found to develop a power law behaviour $\mathrm{Im}\, Z_N \sim \omega^{-\eta_1}$. The exponent $\eta_1 \simeq 0.76$, however, turned out to be substantially larger than the numerical value $\eta \simeq 0.60$ (see section 2).

Improved renormalization schemes can be devised by treating larger cells, but can be carried through only numerically. Consider first the quantity $\Sigma_2(\sigma_i) = Z_2^{-1}$. A renormalized interface conductance $\tilde{\sigma}_2^{(1)}$ is now obtained in analogy to the foregoing discussion by going in figure 6 to the next higher stage of a 16×16 cell. Writing $\tilde{\sigma}_i^{(N-1)}$ for the $(N-1)$ iterate of σ_j, we obtain the second-order approximation

$$Z_{2N}^{-1} = \Sigma_2(\tilde{\sigma}_i^{(N-1)}). \tag{9}$$

Clearly, one could proceed in this manner to higher-order schemes.

Numerical data shown in figure 2 for $N = 2$ are, by construction, identical with $\Sigma_2(\sigma_i)$. An approximation to the data for $N = 4$ is obtained from (9) in the form $Z_4^{-1} = \Sigma_2(\tilde{\sigma}_i^{(1)})$, which is more accurate than the first-order result. We can, however, improve further and use the first-order ($R = 1$) and second-order ($R = 2$) result in an extrapolation to the desired fourth-order result $Z_4^{-1} = \Sigma_4(\sigma_i)$. This is illustrated in the inset of figure 2, which shows a linear extrapolation in the plot $\log(-\sigma_b \mathrm{Im}\, Z_N)$ against the inverse order R^{-1} at a particular frequency. Concerning computing time, this procedure is much faster than the full computation of Z_4. In this way we obtain the full curves in figure 2 for $N = 4$ and, analogously, for $N = 6$. A substantial improvement over the simple first-order scheme is thereby achieved, in particular in the interesting range of intermediate and high frequencies. Exponents η and τ found in this way are $\eta \simeq 0.62$ and $\tau \simeq 0.95$, which compare very well with the full calculation for $N = 4$.

Finally, we indicate an extension of our first-order procedure to disordered interfaces of the type discussed in section 3. The renormalized interface conductance is simply taken as $\sigma_i^{(1)}(p) = (1-p)\sigma_i^{(1)} + p\sigma_i$. This leads to the curves shown in figure 5 in comparison with numerical results.

5. Concluding remarks

We studied the AC response of two-dimensional electrical networks with capacitive coupling to fractal boundaries. Models of this type pertain to the long-standing problem of the dynamic impedance of an electrochemical cell containing a perfectly blocking electrode of irregular shape. Our main objective was to examine the role of different factors determining the CPA exponent η, which characterizes the AC-response at intermediate frequencies. Results for quadratic Koch curve boundaries and modifications thereof suggest the following qualitative analysis. The exponent η is essentially given by interpolating between the high- and low-frequency behaviour of the imaginary part $\mathrm{Im}\, Z_N$. At low frequencies the dependence of this quantity on the stage N in the fractal construction immediately follows from the fractal dimension D of the interface. However, the high-frequency part of $\mathrm{Im}\, Z_N$, which is essentially determined by the protrusions of the boundary, shows non-trivial scaling with the system size L. We verified this observation by numerical simulation and also by renormalization, which was found to agree semiquantitatively with our simulations. Our findings are in accordance with recent work by Halsey and Leibig (1991) and lead to significant deviations from the relation $\eta = 1/D$. On the other hand, comparing boundary geometries with different D but with protrusions of the same geometry, the CPA exponent then varies as $\eta = \mathrm{constant}/D$.

Acknowledgments

Interesting discussions with A Bunde, H E Roman and B Sapoval are gratefully acknowledged. This work was supported in part by the Deutsche Forschungsgemeinschaft, SFB 306.

References

Blender R, Dieterich W, Kirchhoff T and Sapoval B 1990 *J. Phys. A: Math. Gen.* **23** 1225
Chandrasekhar S 1943 *Rev. Mod. Phys.* **15** 1
Geertsma W, Gols J E and Pietronero L 1989 *Physica* **158A** 691
Halsey T C and Leibig M 1991 *Phys. Rev.* A **43** 7087
Le Méhauté A and Crepy G 1983 *Solid State Ionics* **9/10** 17
Meakin P and Sapoval B 1991 *Phys. Rev.* A **43** 7087
—— 1992 *Phys. Rev.* A **46** 1022
Pietronero L and Wiesmann H J 1984 *J. Stat. Phys.* **36** 909
Sapoval B 1991 *Fractals and Disordered Systems* ed A Bunde and S Havlin (Berlin: Springer) p 207
Sapoval B, Gutfraind T, Meakin P, Keddam M and Takenouti H 1993 *Phys. Rev.* E **48** 3333